Journal of Applied Electrochemistry **34**: 797–805, 2004.

Assessment of the wettability of porous electrodes for lithium-ion batteries

MAO-SUNG WU[1]*, TZU-LING LIAO[2] YUNG-YUN WANG[2], and CHI-CHAO WAN[2]
[1]*Materials Research Laboratories, Industrial Technology Research Institute, Hsinchu, Taiwan 310 ROC*
[2]*Department of Chemical Engineering, National Tsing-Hua University, Hsinchu, Taiwan 300 ROC*
*(*author for correspondence, fax: +886-3-5820442, e-mail: ms_wu@url.com.tw)*

Received 13 October 2003; accepted in revised form 19 February 2004

Key words: electrolyte composition, lithium-ion batteries, porous electrode, surface tension, wetting

Abstract

The wettability of lithium cobalt oxide ($LiCoO_2$) and mesocarbon microbead electrodes in nonaqueous electrolyte is analyzed by a mathematical model of capillary liquid movement. Results show that wetting in the $LiCoO_2$ electrodes is difficult as compared with the MCMB electrodes at the same electrolyte composition. Wetting in the porous electrodes is controlled mainly by electrolyte penetration and spreading in pores. Electrolyte penetration is determined by viscosity. On the other hand, electrolyte spreading is controlled by surface tension. Organic solvent composition and lithium salt concentration may influence the wettability of porous electrodes due to changes in the viscosity and surface tension of the electrolyte. Increasing the amount of EC and/or lithium salts can cause poorer electrolyte spreading and penetration. Furthermore, careful pressure control has a positive effect on increasing the surface area of the solid–liquid interface. AC impedance data show that batteries with vacuuming prior to electrolyte filling may reach a maximum wetting in a few hours. If no vacuuming is applied, a few days are required to obtain sufficient wetting.

1. Introduction

Many factors affect the electrochemical performances of lithium-ion batteries. The wettability of the porous electrodes in such cells by the electrolyte is related to capacity and high-rate dischargeability. For example, wetting in a porous electrode with very small pores is problematic, and most of the surface area may not be wetted [1–4]. This results in poor utilization of electrode capacity. In addition, the electrolyte resistance may be increased, thus handicapping high current charging and discharging.

According to Manev et al. [1], when the particle size of graphite powder is larger than 100 μm, the electrolyte resistance is large, especially under rapid charging. But if the graphite powder has been ground, the wetted areas increase due to the decrease in particle radius, and there is also an increase in the capacity at high discharge currents. Menachem et al. [2] used the burn-off method to modify NG7 graphite powder. After treatment, these modified graphites showed better wetting. Furthermore, Manev et al. [3] examined the influence of compacting pressures at electrode preparation on discharge capacity. Experimental results showed that increasing the pressing time leads to a decrease in discharge capacity. This is believed to be due to incomplete wetting of the electrode by lowering the electrode porosity [3, 4].

It is thus important to improve the contacting behavior of the electrode–electrolyte interface in porous electrodes. However, only a few studies mention the effects of electrode porosity or particle size on the wetting in lithium-ion batteries. Measurements of the wettability in mesocarbon microbeads (MCMB) and $LiCoO_2$ electrodes with different electrolyte compositions are scarce. Therefore, this work investigates the interfacial wetting in porous electrodes (MCMB and $LiCoO_2$ electrodes) with varying electrolyte compositions by an average dynamic contact angle method. Effects of physical properties of nonaqueous electrolyte such as viscosity and surface tension on wettability are also studied. Finally, the AC impedance technique is used to analyze the wetting ability in porous electrodes of lithium-ion batteries.

2. Experimental

All electrolytes were prepared in an argon-filled glove box (water content < 2 ppm). Lithium salts were lithium perchlorate ($LiClO_4$, Tomiyama Pure Chemical) and lithium hexafluorophosphate ($LiPF_6$, Tomiyama Pure Chemical) of concentration ranging from 0.2 to 2.0 M. Solvents were ethylene carbonate (EC, Merck) mixed with propylene carbonate (PC, Merck), diethyl

carbonate (DEC, Merck), dimethyl carbonate (DMC, Merck), and γ-butyrolactone (γ-BL, Merck). All electrolytes were tested using a Karl-Fischer instrument (Kyoto Electronics, MKC-510) to ensure that the water content fell below 20 ppm.

Viscosity measurements were carried out using an Ostwald viscometer (Schott Gerate, AVS 310). The Wilhelmy plate method (Face, CBLP-A3) was used to measure the electrolyte surface tension. The substrate was a platinum film of dimensions 24 mm × 15 mm × 0.325 mm. The Wilhelmy plate method was calibrated to ensure accuracy and reliability, with pure water of surface tension 71.2 m N m^{-1} [5]. Prior to testing, electrolyte samples (about 5 cm^3) were placed in a water bath at 30 °C.

For lithium cobalt oxide electrodes, 90 wt % $LiCoO_2$ (20 μm in diameter, Nippon Chemical), 7 wt % KS6 (Timcal SA), and 3 wt % polyvinylidene fluoride (PVDF, Kuraha Chemical) binder were mixed in a solvent of *N*-methyl-2-pyrrolidone (NMP, Mitsubishi Chemical) to form a slurry. The slurry was then coated onto aluminum foil (20 μm in thickness) and dried at 140 °C. Then the electrodes were pressed by rolling and the density of the resultant electrode was 3.2 g cm^{-3}. MCMB electrodes, composed of 92 wt % MCMB (Osaka Gas, 25 μm in diameter) with 8 wt % PVDF binder and NMP, were coated onto copper foil (15 μm in thickness) and were subjected to the same processing steps as the lithium cobalt oxide electrodes. The density of the MCMB electrodes was 1.5 g cm^{-3}. The porosity was measured by mercury porosimetry (Micromeritics, Autopore II9220).

Average dynamic contact angles were measured by the rate of capillary penetration. The apparatus was similar to that for the surface tension measurements, except that platinum foil was replaced by $LiCoO_2$ and MCMB electrodes (2 cm × 5.5 cm). The electrolyte was placed in a water bath at 30 °C for 15 min before measurement.

Test battery samples were assembled in a dry room. The manufacturing process was as follows: the cathode and anode were cut into the appropriate size and wound with the separator to a roll. The roll was then inserted into a stainless steel battery can (cylindrical). The electrolyte was filled into the can and finally the can was sealed. The capacity of such a battery was approximately 500 mA h. In order to prevent negative effects on wetting, the separator was not composed of materials like polypropylene (PP) or polyethylene (PE), but of a copolymer of vinylidene fluoride with hexafluoropropylene (PVDF/HFP).

The capacity tests of the test batteries were carried out by means of charge/discharge unit (Maccor, Series 4000). The electrochemical impedance measurements were taken using a potentiostat/galvanostat (Schlumberger, SI 1286) and a frequency response analyzer (Schlumberger, SI 1255). The scanning frequency ranged from 50 000 to 0.1 Hz. The perturbation amplitude was 10 mV.

3. Results and discussion

3.1. *Wetting in the $LiCoO_2$ and MCMB electrodes*

The model of liquid movement in a capillary can be described by the Washburn equation [6, 7],

$$\frac{dh}{dt} = \frac{r^2}{8\eta h}\left(\frac{2\gamma_{1v}\cos\theta}{r} - \Delta\rho g h\right) \tag{1}$$

where h is the height of liquid penetration at time t, r is the radius of capillary, γ_{1v} is the liquid-to-vapor surface tension, θ is the three-phase contact angle, $\Delta\rho$ is the difference in density between the liquid and the gas-phase, and η is the viscosity. In a porous electrode, irregularity of the pores is taken into account and the radius of capillary, r, is replaced by the effective radius, $\overline{r_{\text{eff}}}$. Thus, the above equation refines to

$$\frac{dh}{dt} = \frac{\overline{r_{\text{eff}}^2}}{8\eta h}\left(\frac{2\gamma_{1v}\cos\theta}{\overline{r_{\text{eff}}}} - \Delta\rho g h\right) \tag{2}$$

Equation 2 can be further reduced, if $\overline{r_{\text{eff}}}$ is very small or if gravity is ignored, to

$$\frac{dh}{dt} = \frac{\overline{r_{\text{eff}}}\,\gamma_{1v}\cos\theta}{4\eta h} \tag{3}$$

Assuming $t = 0$ and $h = 0$, the integrated equation can be re-written as [7]

$$h = k\sqrt{t}, \quad k = \sqrt{\frac{\overline{r_{\text{eff}}}\gamma_{1v}\cos\theta}{2\eta}} \tag{4}$$

where k is a combination of the effective radius, surface tension, viscosity, and three-phase contact angle, and can be referenced as the penetration ability of a liquid—the coefficient of penetration or penetrability. The higher the k, the faster the flow of liquid within a porous substrate.

The height of liquid penetration, h, may be defined with the cross-section area of electrode (A_e) and electrode porosity (P) as follows [7]

$$h = \frac{1}{\rho A_e P}\Delta m \tag{5}$$

where Δm is the measured mass increase, ρ is the density of the electrolyte. When combined with Equation 4, the equation becomes as follow

$$\frac{\Delta m}{\rho} = K\sqrt{t}, \quad K = \sqrt{\frac{\overline{r_{\text{eff}}}\gamma_{1v}\cos\theta}{2\eta}}A_e P \tag{6}$$

In the first part of Equation 6, the total amount of liquid penetrating into a substrate displays a linear relationship with the square root of t and a slope of K. The value of K represents the speed of liquid penetration. From the

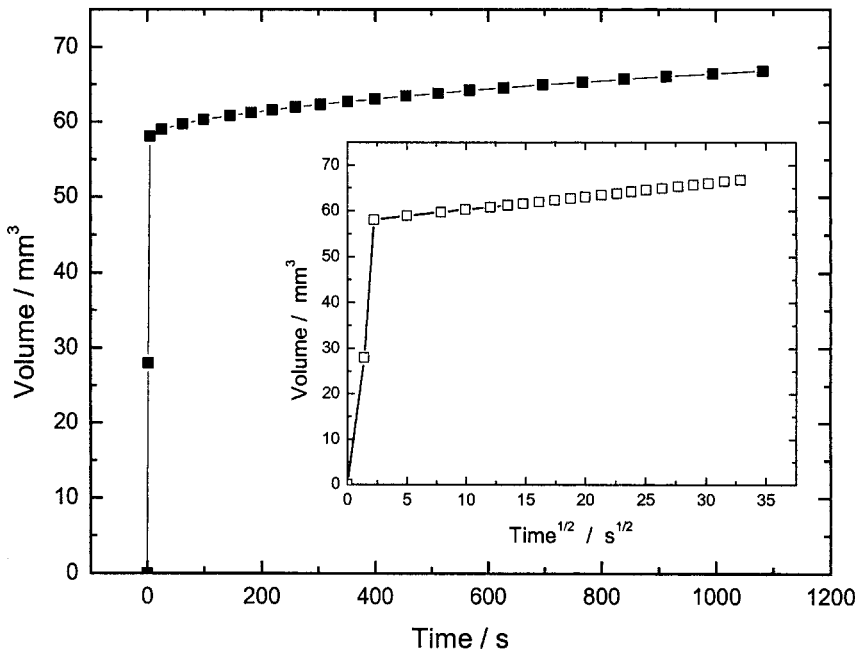

Fig. 1. Change in measured electrolyte volume with respect to time and to square root of time (inset) after electrolyte contact. The electrolyte was composed of 1:1 (by volume) EC and DMC with 1 M $LiClO_4$.

equation, the average dynamic contact angle can then be calculated if other parameters are known. Figure 1 shows the relationship between the electrolyte penetration volume and time of the MCMB electrodes. Changes in the first 5 s are most drastic, induced mainly by the solid–liquid interfacial surface tension. The moderate increase in volume after 5 s is then the actual volume of liquid penetrating.

To determine the effective radius, a liquid with smaller surface tension was chosen. Assuming that the contact angle approaches 0°, the effective radius may be calculated by using Equation 6. DEC, an organic solvent with small surface tension ($\rho = 0.9752$ cm^3 g^{-1}, $\gamma = 26.4$ m N m^{-1}, and $\eta = 0.748$ mPa s) [8], was chosen for the calculation of effective radii in the MCMB and $LiCoO_2$ electrodes. Penetrability of DEC in the MCMB (porosity 24.75%) and $LiCoO_2$ (porosity 22.58%) electrodes were 0.4101 mm^3 s$^{-1/2}$and 0.2548 mm^3 s$^{-1/2}$, respectively, therefore $\overline{r_{\text{eff}}}$ were 0.108 and 0.053 μm.

In practical use, the electrolyte used in lithium-ion batteries is not composed of a single component such as DEC but of a mixture of organic solvents and lithium salts. Electrolyte composition greatly influences the wettability of porous electrodes in lithium-ion batteries because the electrolyte physical properties such as viscosity and surface tension change as the composition changes. Figure 2 shows the viscosity curves of organic solvents at different compositions. Changes in a solvent viscosity without lithium salts are small. Viscosity depends on the composition. EC/γ-BL, EC/DEC, and EC/DMC systems all show a similar trend of viscosity increase directly proportional to EC amount, but the viscosity of EC/PC decreases slightly. It is generally accepted that the addition of lithium salts may change the viscosity of electrolyte [9, 10]. Figure 3 shows viscosity curves of the electrolyte at different salt additions and solvent compositions. Apparently viscosity increases as the salt concentration increases, with either $LiClO_4$ or $LiPF_6$ addition. According to Prabhu et al. [9], this increase is due to a structural enhancement through the formation of a solvated complex. Another physical property, which influences the wettability of porous electrodes, is the surface tension. Figure 4 shows the changes in surface tension with varying EC concentration in different solvents. All electrolyte systems show a trend of increasing surface tension with increasing EC. Surface tension is believed to depend on the polarities of the organic solvent: the larger the polarity, the larger the surface tension. Because EC has a large polarity, it is reasonable to obtain experimentally an increase in the surface tension with increasing EC concentration. Figure 5 shows the changes in surface tension with respect to the salt concentrations, and the changes are small. The surface tension increases approximately 3–4 m N m^{-1}, when the salt concentration varies from 0.2–2.0 M. Therefore, bulk properties (i.e. viscosity) of a solvent mixture may change with the addition of salts but no obvious variation in the surface properties (i.e. surface tension) is observed. Accordingly, the surface tension is influenced mainly by the organic solvent compositions.

Figure 6(a) shows the penetrability, K, of different organic solvents in the $LiCoO_2$ electrodes. Regardless of the solvent compositions, K is inversely proportional to EC concentration. Similar trends may also be found in the MCMB electrodes (Figure 6(b)). When the EC concentration remains constant, the magnitude of K is in the order of DMC > DEC > γ-BL > PC. Penetrability is depended on the effective radius ($\overline{r_{\text{eff}}}$), surface

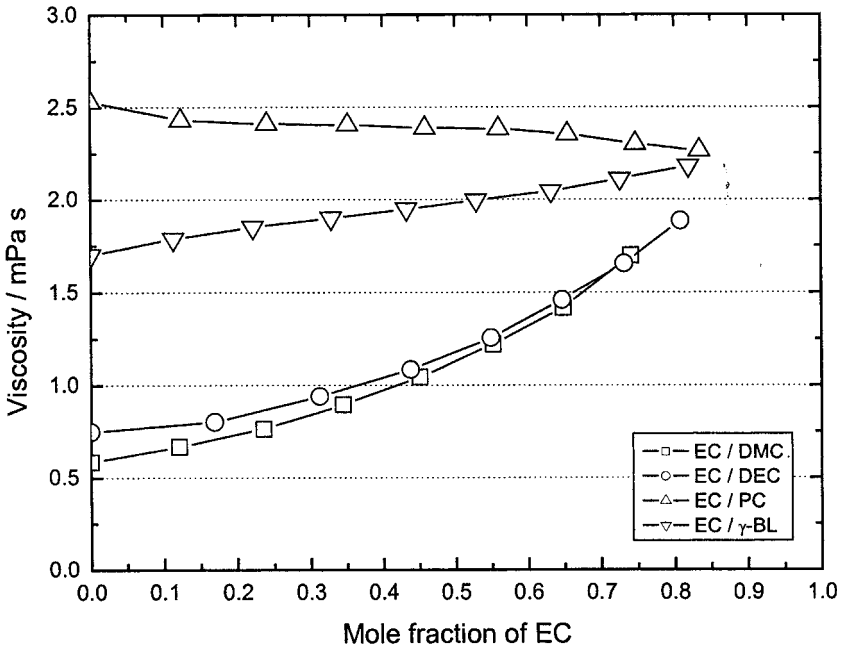

Fig. 2. Viscosity curves of organic solvents at different compositions.

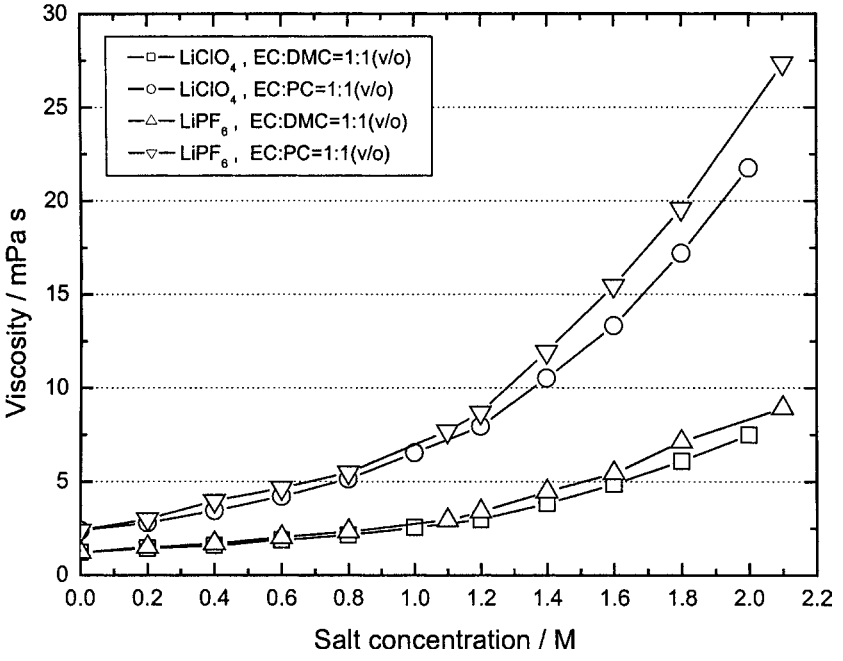

Fig. 3. Viscosity curves of electrolyte at different salt additions and solvent compositions.

tension (γ_{lv}), contact angle (θ), and viscosity (η) (Equation 6). In a substrate, $\overline{r_{eff}}$ is fixed which leaves the other parameters variable. $\gamma_{lv} \times \cos\theta$ may be regarded as the interfacial force to be distinguished from viscosity. According to the capillary theory, increasing $\gamma_{lv} \times \cos\theta$ enhances liquid penetration; and when the contact angle is equal to 0°, $\gamma_{lv} \times \cos\theta$ reaches its largest value and equals the surface tension. On the other hand, an increase in viscosity hinders liquid penetration. Experimentally, both the viscosity and surface tension of EC/DMC, EC/DEC, and EC/γ-BL show an increasing trend as the EC concentration increases; but the penetrability decreases. Although the viscosity of EC/PC remains constant, its surface tension follows the increasing pattern. These combinations of electrolytes are theoretically advantageous in speeding up the liquid penetration, though experimental results show otherwise: K stays unchanged. That is, for organic solvents in lithium-ion battery systems, even when the interfacial force reaches its maximum, viscosity still is the controlling factor. In addition to the organic solvent compositions, additives of lithium salts are also influential to

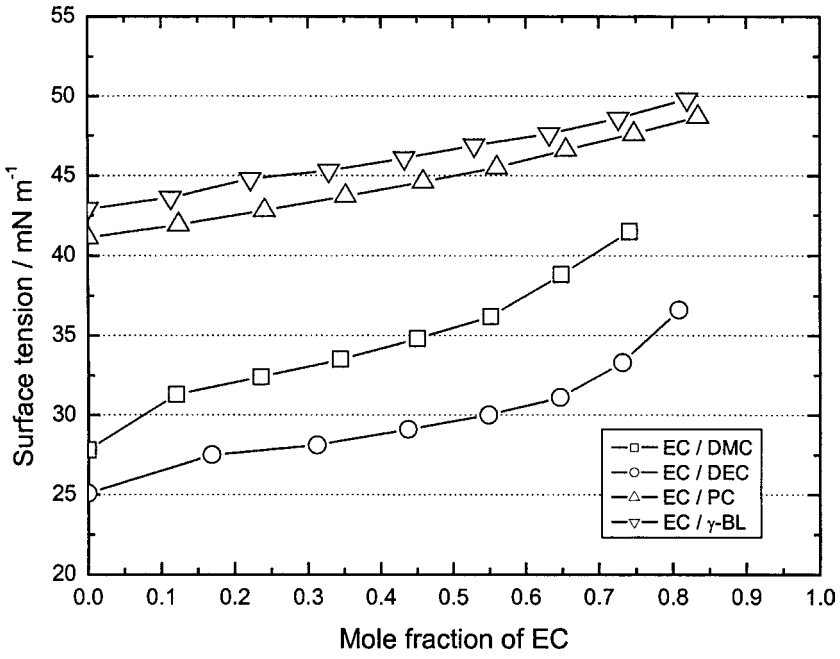

Fig. 4. Changes in surface tension with varying EC concentration in different solvents.

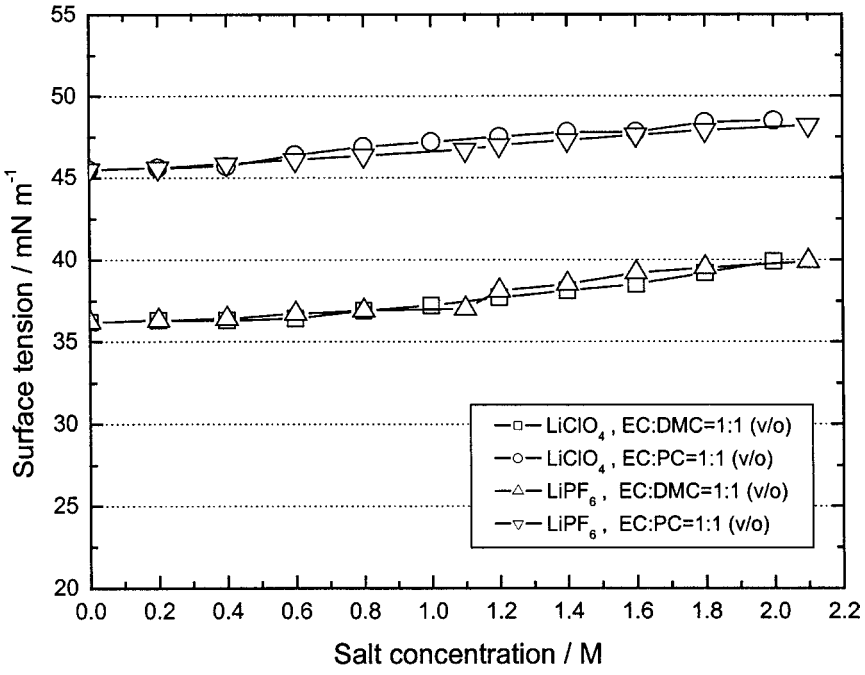

Fig. 5. Changes in surface tension with respect to salt concentrations.

the electrolyte properties. Effects of lithium salts addition on the penetrability are shown in Figure 7(a) and (b). Although salt concentrations do not affect surface tension much, significant increases in viscosity by as much as 6–10 times may result as the concentration increases, leading to a decrease in *K*-value. In other words, the electrolyte penetrability can be drastically decreased with increase in salt concentration. A difference between the MCMB and $LiCoO_2$ electrodes is that the latter has a lower *K*-value in general. $\overline{r_{\text{eff}}}$ of the two electrodes are calculated as 0.108 and 0.053 μm; however readings from mercury porosimetry are 1.2 and 0.3 μm, respectively. This difference is mainly caused by the powder properties of the electrodes. Pores in electrodes are not evenly capillary but zigzagging, thus enhancing up resistance to wetting by solvents.

Figure 8(a) shows the relationship between the contact angles and the compositions of organic solvents in

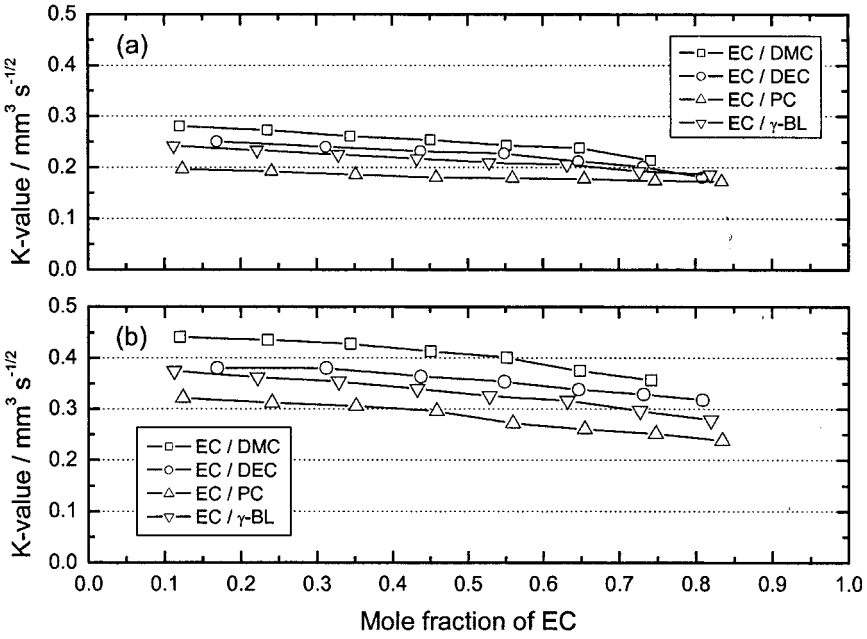

Fig. 6. Penetrability (K) of different organic solvents in (a) $LiCoO_2$ and (b) MCMB electrodes.

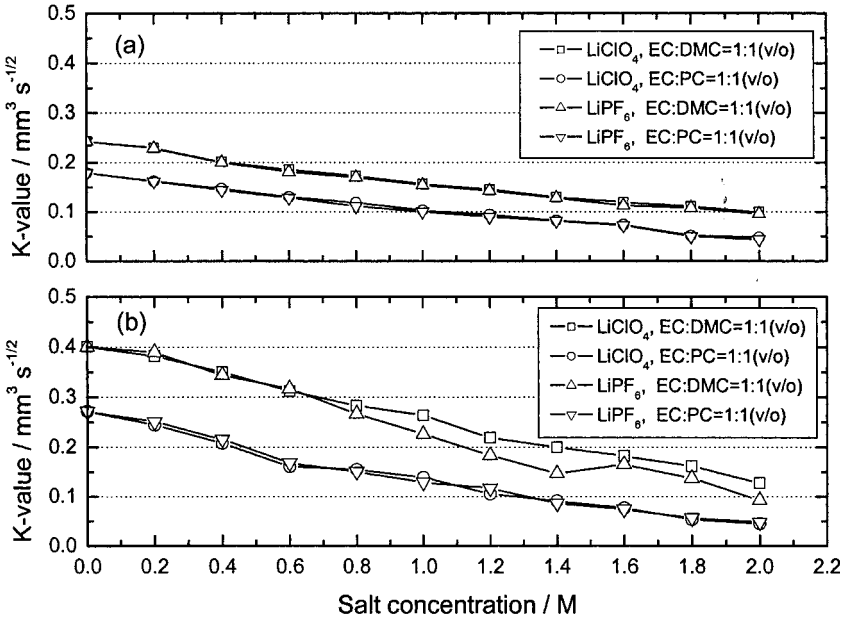

Fig. 7. Penetrability (K) of different salt concentrations in (a) $LiCoO_2$ and (b) MCMB electrodes.

the $LiCoO_2$ electrodes. Independent of the solvent compositions, trends in which the contact angles increase with increasing EC concentrations are all similar. A similar trend is also found in the MCMB electrodes, shown in Figure 8(b). Similarly, increasing trends of contact angles are observed when the salt concentrations are increased. The higher the salt concentrations, the higher the measured contact angles (Figure 9(a) and (b)). However, increase in contact angle means less wetting in the electrodes. Therefore, an increase in the EC concentration and/or lithium salt concentration leads to a decrease in wettability. Amongst all, contact angle has a trend of EC/PC > EC/γ-BL > EC/DMC > EC/DEC (Figure 8), and is larger in PC than in DMC regardless of the electrodes used at the same salt concentration (Figure 9). The increase in surface tension causes the contact angle to increase, thus reducing electrolyte spreading on the interface.

3.2. *Relation between wetting and time*

Figure (10)a shows the changes in the AC impedance of a battery with respect to time after electrolyte filling.

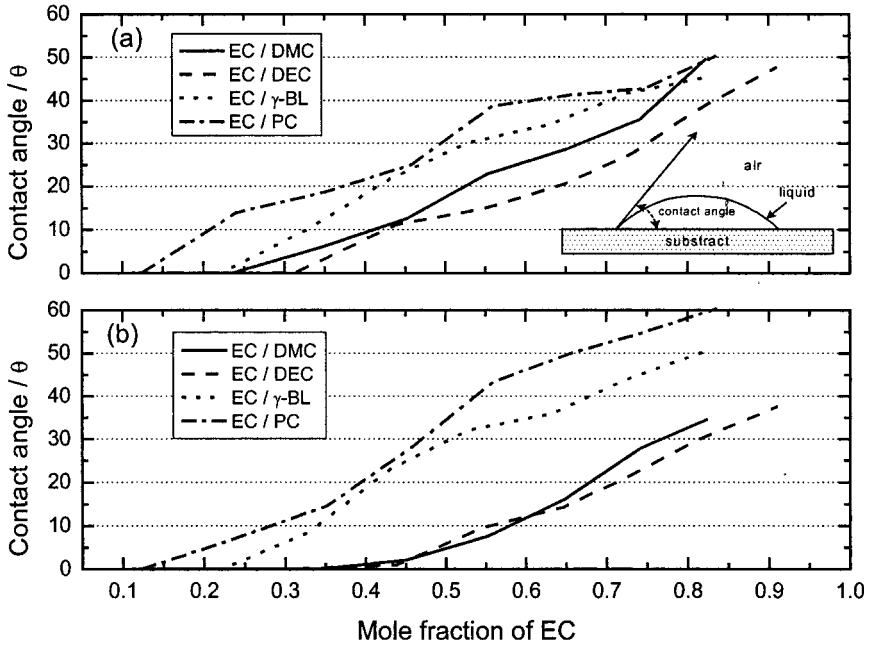

Fig. 8. Relationship between contact angles and compositions of organic solvents in (a) $LiCoO_2$ and (b) MCMB electrodes.

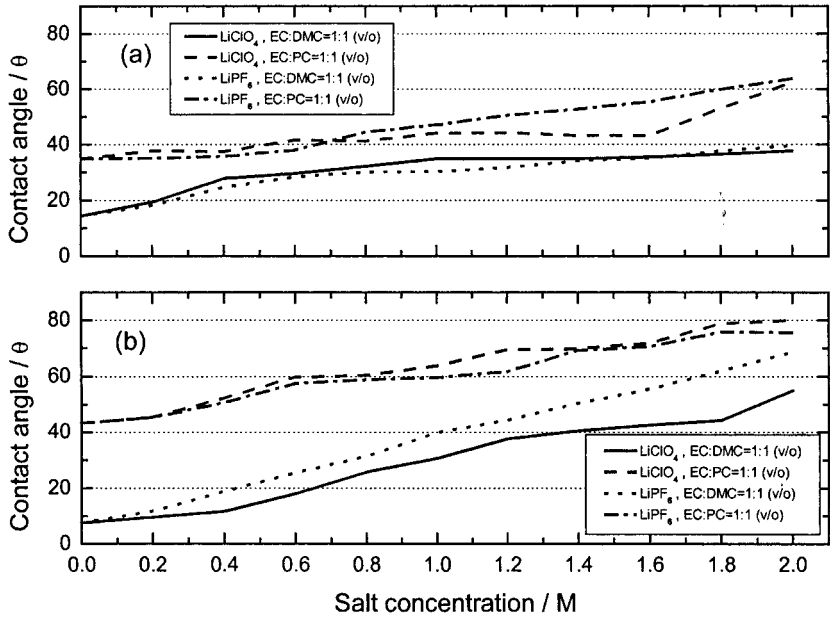

Fig. 9. Relationship between contact angles and salt concentrations in (a) $LiCoO_2$ and (b) MCMB electrodes.

Interceptions in the high-frequency range are directly related to the conductivity of the electrolyte. Electrolyte conductivity is often calculated by using the following equation,

$$\sigma = \frac{1}{R} \times \frac{L}{A} \tag{7}$$

where σ is the electrolyte conductivity, R is the resistance obtained from the intercept in Figure 10a, A is the electrode surface area, and L is the distance between electrodes. Clearly, from the Figure 10(a), the intercept decreases with increasing wetting time. Variation in the electrolyte conductivity, σ, is negligible because measurements were taken at a constant temperature (30 °C). The distance between electrodes, L in Equation 7, is also fixed, hence the relationship between the electrode area (A) and the resistance (R) may be changed to,

$$R \times A = \frac{L}{\sigma} = \text{constant} \tag{8}$$

Therefore according to Equation 8, a decrease in resistance corresponds to an increase in electrode area,

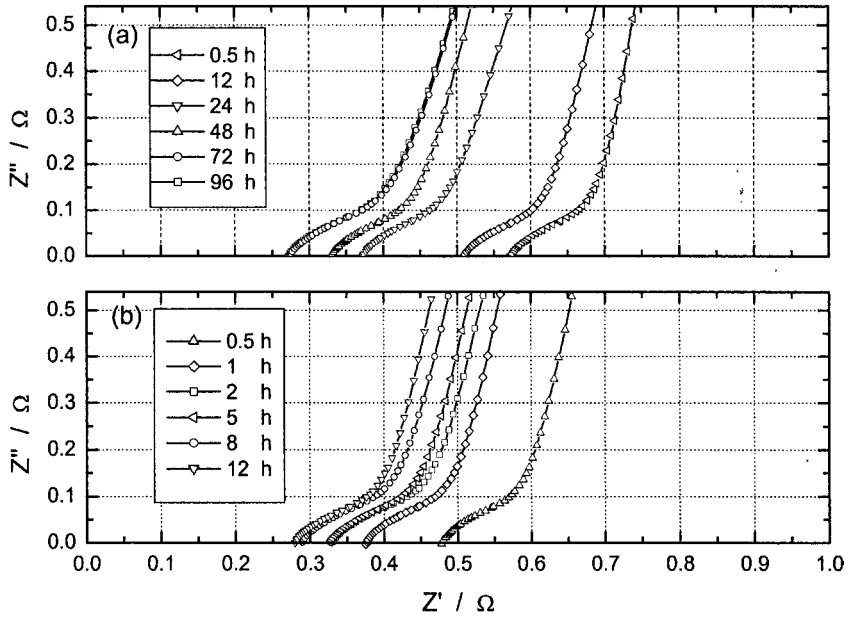

Fig. 10. Changes in Nyquist plots of a battery with respect to time in which electrolyte is filled after (a) no vacuuming and (b) vacuuming. The electrolyte was composed of 2:1 (by volume) EC and PC with 1 M $LiPF_6$.

meaning that the interface of wetted electrode by electrolyte in Figure 10a increases. The stabilized resistance indicates a maximum wetting of electrode pores.

3.3. *Effect of pressure on wetting*

Prior to the electrolyte filling, batteries are vacuumed in a chamber (end pressure was approximately 60 mmHg). Filling was done within the same vacuumed chamber through a pipe. Generally, surface tension decreases with increasing pressure and vice versa. Therefore the surface tension increases under vacuum condition which, in turn, increases penetrability. However, the contact angle also increases as a result of vacuum and obstructs the interaction between solid and liquid. Figure 10b shows the changes in the AC impedance of a battery that was vacuumed prior to the electrolyte filling. Both Figure 10(a) and (b) results were taken 30 min after assembly. The curve for the vacuumed battery has a smaller intercept value. Therefore wetted area in the electrode may actually be increased if the pressure is systematically controlled. The change in impedance is faster for a vacuumed battery and the resistance stabilizes within a few hours; whereas, a battery without vacuuming requires approximately 3 days to reach the same condition. Results not only show that pressure may affect the penetrability of electrolyte in the porous electrodes, but also suggest that as the surface tension increases during vacuuming, the wetted area is enlarged. The area increased by the high penetrability is larger than the area decreased by the increased solid–liquid contact angle. Theoretically, liquid penetration into electrode pores is easy at low pressure, however the results show at least a few hours is required to reach the maximum wetting. There are two possibilities to this time requirement. First, although the battery has been vacuumed prior to electrolyte filling, there still remains some gas in the pores and in the spaces between the tightly packed electrodes and separator. The second possibility is that during electrolyte filling, organic solvents evaporate instantaneously into the pores and become obstacles for penetration. The wetting speed is therefore not as fast as expected. Lastly, an experiment was done on electrolyte filling under vacuumed and un-vacuumed conditions to compare the discharge capacities at different currents, as shown in Figure 11. A vacuumed battery has a higher capacity and may still retain approximately 300 mA h at 1200 mA discharge while the battery without vacuuming does not even discharge satisfactorily.

4. Conclusion

Wetting of the porous electrodes is controlled by electrolyte penetration and spreading. Penetration behavior in the $LiCoO_2$ and MCMB electrodes is mainly controlled by the viscosity of the electrolyte. Change of the organic solvent does not have a pronounced effect on viscosity, but change in the lithium salt increases viscosity. Spreading behavior in the $LiCoO_2$ and MCMB electrodes is determined by the average dynamic contact angle. Electrolyte spreading is related to the surface tension. The greater the surface tension, the larger the contact angle. Both EC and lithium salts may increase the surface tension, therefore obstructing solid–liquid interface spreading. In addition to the electrolyte, properties the environment is also important. The AC impedance analysis shows that batteries with vacuuming prior to electrolyte filling

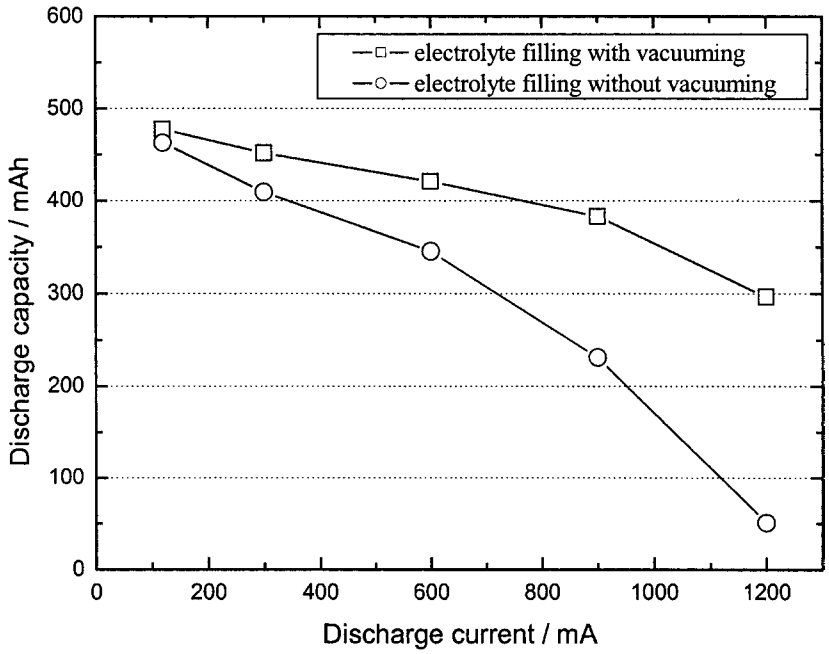

Fig. 11. Relationship between discharge capacities and discharge currents at different electrolyte filling conditions. The electrolyte was composed of 2:1 (by volume) EC and PC with 1 M $LiPF_6$.

may reach maximum wetting in a few hours; they have higher capacities and are not as sensitive to high current discharge. On the other hand, for batteries without vacuuming, a few days duration is required to reach stability, and generally they have lower capacities and decay rapidly when discharged at high current. Thus, a careful pressure control has positive effects on increasing the surface area of the solid–liquid interface.

References

1. V. Manev, I. Naidenov, B. Puresheva, P. Zlatilova and G. Pistoia, *J. Power Sources* **55** (1995) 211.
2. C. Menachem, E. Peled, L. Burstein and Y. Rosenberg, *J. Power Sources* **68** (1997) 277.
3. V. Manev, I. Naidenov, B. Puresheva and G. Pistoia, *J. Power Sources* **57** (1995) 133.
4. P. Novák, W. Scheifele, M. Winter and O. Hass, *J. Power Sources* **68** (1997) 267.
5. D.R. Lide, 'Handbook of Chemistry and Physics', 74th edn (CRC Press, Boca Raton, FL, 1997).
6. E.W. Washburn, *Phys. Rev.* **17** (1921) 374.
7. A. Lundblad and B. Bergman, *J. Electrochem. Soc.* **144** (1997) 984.
8. J. Brandrup and E.H. Immergut, 'Polymer Handbook', 3rd edn (John Wiley & Sons, New York, 1989).
9. P.V.S.S. Prabhu, T.P. Kumar, P.N.N. Namboodiri and R. Gangadharan, *J. Appl. Electrochem.* **23** (1993) 151.
10. K. Kondo, M. Sano, A. Hiwara, T. Omi, M. Fujita, A. Kuwae, M. Iida, K. Mogi and H. Yokoyama, *J. Phys. Chem. B* **140** (2000) 5040.